https://doi.org/10.5194/egusphere-2026-3608
Preprint. Discussion started: 30 June 2026

Lead isotopes in deep sea sediments reveal alteration of the isotopic composition signal in the water column at highly productive sites in the South Atlantic Ocean

Lina Oskamp[1], Marta Pérez Rodríguez[1], Adelina Calean[1], Olaf Rienitz[2], Klaus-Holger Knorr[3], Kazumasa Oguri[4], Masashi Tsuchiya[5], Marco Benkhettab Sindlev[4], Stephan Krisch[1], Arianna Olivelli[6], Frank Wenzhöfer[4,7], Ronnie N. Glud[4,8,9], Harald Biester[1*]

[1] Institute for Geoecology, TU Braunschweig, Braunschweig, 38106, Germany
[2] Physikalisch-Technische Bundesanstalt (PTB), Braunschweig, 38116, Germany
[3] Institute of Landscape Ecology, University Münster, Münster, 48149, Germany
[4] HADAL & Nordcee, University of Southern Denmark, Odense, 5230, Denmark
[5] Faculty of Dinosaur Paleontology, Fukui Prefectural University, Fukui, 910-1142 Japan
[6] Flanders Marine Institute (VLIZ), Ostend, 8400, Belgium
[7] HGF MPG Joint Research Group for Deep-Sea Ecology and Technology, Max Plank Institute for Marine Microbiology, Bremen, 28359, Germany
[8] Danish Institute for Advanced Study (DIAS), University of Southern Denmark, Odense, 5230, Denmark
[9] Department of Ocean and Environmental Sciences, Tokyo University of Marine Science and Technology, Tokyo, 108-8477, Japan

[*] **Correspondence to Harald Biester (h.biester@tu-braunschweig.de)**

https://doi.org/10.5194/egusphere-2026-3608
Preprint. Discussion started: 30 June 2026

Abstract

Lead (Pb) isotope fingerprints in marine sediments are frequently used as tracers of natural or anthropogenic Pb sources. This assumes that Pb isotope ratios are not altered within the water column or sediments. Recent studies suggest reverse scavenging of Pb isotopes by biogenic particles during sinking through the water column, but it remains unclear if and how this affects the Pb isotope signal in deep sea sediments. This study examines Pb isotope records ($^{206}Pb/^{207}Pb$ and $^{208}Pb/^{207}Pb$) in pelagic sediments of a highly productive area in the South Atlantic Ocean and their relation to primary productivity as reflected by the silicon (Si) and total organic carbon (TOC) contents. Three cores were extracted at three different stations northwest and southeast of South Georgia and at different water depths (St9: 3796 m, St15: 8066 m, and St16: 5002 m). Downcore Pb and total organic carbon concentrations ranged from 4 to 12 µg g^{-1} and from 0.17 to 0.89 % respectively, with highest Pb concentrations in the core taken at the deepest water depth. Lead isotope signatures reflected Patagonian dust as the major Pb source. Lead isotope ratios in the sediment cores were generally larger than those of dissolved Pb in the water phase observed in previous studies, indicating a separation between Pb isotope pools in the water column. Distinct variations in Pb isotope ratios correlated with the content of Si and TOC, indicating an influence of primary productivity on Pb scavenging in the water column. Correlations of Pb concentrations and isotope ratios with TOC content were most pronounced at the deepest sampling station, but were less distinct at other stations presumably due to dilution by biogenic Si. Besides implications on the biogeochemical Pb marine cycle, our findings question the use of Pb isotope signatures in deep sea sediments for source tracing. Future studies combining water phase, particulate matter and sediment Pb isotope analyses should address how signatures of Pb isotope ratios are altered in the water phase during sinking and investigate fractionation processes during Pb burial in deep sea sediments.

https://doi.org/10.5194/egusphere-2026-3608
Preprint. Discussion started: 30 June 2026

1 Introduction

Anthropogenic perturbations of the natural lead (Pb) cycle exceed natural sources by a factor of 25 – 30 (Boskabady et al., 2018). The natural flux of Pb to the oceans through continental runoff is estimated at 295 000 t a^{-1} (Cullen and McAlister, 2017; Henderson and Maier-Reimer, 2002), with additional contributions from natural Pb emission into the atmosphere, such as volcanic activity and airborne soil and crustal dust (Nriagu and Pacyna, 1988). However, since the industrial revolution, atmospheric inputs have been the major source of Pb into the oceans (Chen et al., 2016; Veron et al., 1993; van de Flierdt et al., 2003; Weiss et al., 2003). Productive coastal zones used to act as a barrier for Pb from riverine sources through scavenging of Pb onto particulate matter, leading to Pb deposition in hemipelagic sediments. However, direct atmospheric deposition onto the surface ocean introduces Pb across a wide area, subjecting Pb inputs to lateral transport via ocean currents (Samanta et al., 2023; Krisch et al., 2025). On decadal to centennial timescales, this Pb input propagated also into deep ocean environments in the remotest regions of the global oceans (Boyle et al., 2014; Gobeil et al., 2001; Olivelli et al., 2025; Bridgestock et al., 2018). Anthropogenic Pb emissions were thus transferred into the ocean interior by thermocline ventilation, deep-water formation and transport with natural and anthropogenic particles (Lalande et al., 2016). Transport to depth occurs through scavenging of Pb onto particles (Lalande et al., 2016; Griffiths et al., 2026). This process may involve the flocculation of organic metal colloids (Yang et al., 2015), manganese (Mn) and iron (Fe) oxides, and the aggregation of organic particles from phytoplankton blooms, including organic debris and fecal pellets (Turekian, 1977; Iseki, 1981; Tanguy et al., 2011). Hence, biologically active particles influence Pb distribution, making zones of high surface primary productivity hot-spots for Pb removal from the water column (Cullen and McAlister, 2017; Henderson and Maier-Reimer, 2002; Griffiths et al., 2026). Pelagic sediments thus act as the ultimate sinks, and a large repository for Pb (Hesse and Schacht, 2011).

Stable isotope ratios of Pb have been widely employed as tracers for discerning its sources across environmental compartments, assuming that secondary changes of Pb isotope composition in the environment are negligible (Komárek et al., 2008; Zurbrick et al., 2017). While phase exchange of Pb isotopes was detected in closed system experiments (Chen et al., 2016) and in the ocean water column (Lanning et al., 2023), mass dependent fractionation of Pb isotopes has not yet been observed, neither in

https://doi.org/10.5194/egusphere-2026-3608
Preprint. Discussion started: 30 June 2026

laboratory experiments, nor in field studies. Unlike for other elements like nickel (Ni) (Yang et al., 2020), physio-chemical fractionation is assumed not to play a major role for Pb isotopes, as the large elemental mass and consequently small weight differences between isotopes preclude large mass-dependent fractionation effects through thermal diffusion or adsorption (Doe, 1970; Komárek et al., 2008). Chen et al. (2016a) suggested that all Pb isotopes move between their sub-reservoirs at effectively the same rate, with any mass-dependent differences in rate being negligible (Chen et al., 2016), ruling out mass-dependent Pb isotope fractionation.

Most studies on the distribution of Pb isotopes in the oceans are based on water column sampling of dissolved (Chen et al., 2023; Olivelli et al., 2025; Bridgestock et al., 2018; Veron et al., 1993; Boyle et al., 2014) or total dissolvable Pb (Bridgestock et al., 2018; Olivelli et al., 2025). Studies on Pb isotopes in sediments, specifically in the open ocean, are still rare (Larsen et al., 2012; Shi et al., 2022). Moreover, the extent to which Pb isotope exchange processes between dissolved Pb and sinking particulate matter occur in the water column and how this influences the Pb isotopes signal preserved in deep sea sediments remains largely unclear. In a recent study, the exchange of Pb isotopes between water and particle phases revealed equilibration of Pb isotope ratios from their initial aerosol values to more geogenic values through exchange processes involving crustal particulates (Chen et al., 2016). Pb isotope exchange between sub-reservoirs is thus possible without changes in concentrations, re-equilibrating isotope ratios in dissolved and particulate phases (Chen et al., 2016; Lanning et al., 2023). Changes in isotope composition would thus not merely be a result of source mixing processes as assumed by (Cheng and Hu, 2010), but also of isotope exchange processes.

Recently, several indications for Pb isotope exchange processes in the ocean's water phase related to sinking particles have arisen (Chen et al., 2016; Lanning et al., 2023). Lanning et al. (2023) and Wu et al. (2010) found evidence for reversible scavenging, i.e. the re-dissolution of previously adsorbed Pb along the water column in the North Pacific. The study of Lanning et al (2023) has shown that reversible scavenging and alteration of water column Pb isotope composition is most intense in highly productive areas and that reversible scavenging is transporting anthropogenic Pb down to deep water masses. Olivelli et al. (2024) investigated depth profiles of dissolved Pb isotopes in the water column along a north-south and west-east transect (5 °S to 50 °S and 60° W to 20° E) in the South Atlantic and found that in low

https://doi.org/10.5194/egusphere-2026-3608
Preprint. Discussion started: 30 June 2026

productivity regions, Pb isotope fingerprints are consistent with the traditional interpretation that water column variability reflects advective transport of different water masses bearing Pb isotope signatures derived from geographical origin. However, in areas with high particulate matter loads, vertical transport of anthropogenic Pb by marine particles in combination with reversible scavenging alters the advected Pb isotope signature and may invalidate the use of Pb isotopes as transient tracers of water masses (Olivelli et al., 2024). Furthermore, it has been argued that in areas where particulate matter loads are high, sedimentary records of Pb isotopes might reflect the occurrence of vertical rather than advective Pb transport (Schlosser et al., 2019), with particle composition assumed to act as major influence on Pb transport to the deep ocean (Griffiths et al., 2026). However, none of these studies examined Pb isotope composition of particulate matter and, therefore, it remains unclear how Pb isotope signatures in the dissolved phase and in particulate matter compare and what signature is exported to the sediment. Moreover, existing studies assume that Pb scavenging occurs, although it is not known whether it is restricted to the mixed layer where particulate matter loads are highest or occurs in the entire water column (Lanning et al., 2023; Olivelli et al., 2024; Schlosser and Garbe-Schönberg, 2019; Schlosser et al., 2019), and whether Pb isotope signatures in biogenic particulate matter are altered during sinking through the water column exposed to both decomposition and increasing pressure.

In this study, we investigate Pb isotope ratios ($^{206}Pb/^{207}Pb$, $^{208}Pb/^{207}Pb$) and Pb concentration records in pelagic sediments collected from three stations at depths of water column ranging from 3500 to 8066 m in the South Atlantic Ocean (SAO), specifically in the Scotia Sea (51° and 56° S and 24° to 40 W°). We assess the relationship between Pb isotope signatures and variations in Si and organic carbon content, which serve as proxies for organic matter accumulation in the sediments and associated changes in primary production in the oceans mixed layer. We further aim to disentangle the influence of productivity driven particulate matter flux on Pb isotope signature deposition in sediments. We hypothesize that sedimentary Pb isotope signatures overlap with regional seawater Pb isotope compositions and are modified by variations in upper ocean primary productivity. Our focus is on the $^{206}Pb/^{207}Pb$ and $^{208}Pb/^{207}Pb$ isotope ratios since they have been commonly used for Pb source tracing in ocean environments (Komárek et al., 2008).

https://doi.org/10.5194/egusphere-2026-3608
Preprint. Discussion started: 30 June 2026

2 Materials & Methods

2.1 Sampling

In November 2022, sediment cores were collected in the South Atlantic Ocean during the Polarstern cruise PS133/1 as part of the Island Impact and South Polar Carbon Projects lead by C. Klass and S Karsten, R. N. Glud and F. Wenzhöfer, respectively. Undisturbed sediment cores of varying lengths (12 - 24 cm) were recovered from three stations at water depths between 3000 and 8000 m using a multicorer (MUC). St9 (51°18'04.3"S, 39°55'31.2"W) is located within the South Georgia Basin, a highly productive area of the SAO (Soppa et al., 2016) at 3795.8 m depth. St15 (55°13'52.3"S, 26°10'15.6"W) is located at the deepest point of the South Sandwich Trench (i.e., Meteor Deep, 8066.4 m depth), and St16 (55°48'02.9"S, 24°50'20.6"W) is located on the rim of the South Sandwich Trench at 5002 m depth. For net primary productivity (NPP) data in the surface water, see Table S1, SI. The cores were sectioned on board in a cold room into 1 cm intervals from 1 to 10 cm depth, 2 cm intervals from 10 to 20 cm, and 5 cm intervals below 20 cm and kept frozen at -18 °C for transport. Sample preparation was conducted at the Environmental Geochemistry laboratory at Technische Universität Braunschweig, where sediment samples were freeze-dried (VaCo 2 freeze-drier by Zirbus) and homogenized.

2.2 Pb isotope measurement

Pb isotope measurements were carried out at the Physikalisch-Technische Bundesanstalt (PTB, Braunschweig, Germany) between July 7 and August 8, 2025, using a Neptune XT multi-collector inductively coupled plasma mass spectrometer (MC-ICP-MS) Neptune XT (Thermo Fisher Scientific, Bremen, Germany). Samples of 0.15 g to 0.6 g were digested using 9 mL 65 % HNO_3 (subboiled twice, Roth ROTIPURAN® p.a., Carl Roth GmbH + Co. KG, Karlsruhe, Germany), 4 mL 48 % HF (Roth ROTIPURAN® Supra), and 3 mL 25 % HCl (subboiled twice, Bernd Kraft, AnalytiChem, Duisburg, Germany) in an ETHOS.lab microwave system (MLS GmbH, Leutkirch, Germany) within 2 h at 210 °C. After cooling down, the solutions were evaporated to complete dryness. 15 mL of 1 mol/L HNO_3 (subboiled twice, Roth ROTIPURAN® p.a.) were added to the residues. 2 × 4 mL of the resulting clear and colorless solutions were loaded onto preconditioned 2 mL pre-packed resin columns PB-C20-A (Triskem International, Bruz, France, Lot # FPBA230215) for a matrix separation (Table S3, SI). To

https://doi.org/10.5194/egusphere-2026-3608
Preprint. Discussion started: 30 June 2026

remove the HCl, the tubes were put in an aluminium heating block on a hot plate at 120 °C for approximately 30 h. The residues (containing column material abrasion) were redissolved in 3 mL 65 % HNO_3 (subboiled twice, Roth ROTIPURAN® p.a.) and evaporated to dryness within 8 h using the Al heating block on a hotplate at a surface temperature of up to 150 °C. The resulting residues were redissolved in 15 mL of 1 mol L^{-1} HNO_3 (subboiled twice, Roth ROTIPURAN® p.a.) to yield measurement solutions with a lead content of approximately w(Pb) ≈ 100 ng g^{-1}. The sample solutions were filtered through PTFE filter discs with 0.45 µm pore diameter (Chromafil Xtra GF/PTFE-45/25, Macherey-Nagel GmbH & Co. KG, Düren, Germany) using 10 mL Luer-lock PE syringes (BD Dicardit II, Becton Dickinson S.A., Fraga, Spain) directly into the pre-cleaned 4 mL PFA autosampler vials (Cetac, Omaha, USA). All measurements were performed using a MC-ICP-MS in low resolution mode (M/ΔM = 450) with a plasma power of 1200 W (Table S5, SI). At the beginning and end of each sequence (45 measurements), an acid blank and a procedural blank were measured. Within the sequence, four sample measurements were always bracketed by measurements of the isotope reference (NIST SRM 981). The measurements of the isotope references showed an average relative uncertainty of < 0.0030 % (n = 9) and were corrected for the acid blank while processed samples were corrected for the procedural blank, when calculating the isotope ratios. The reproducibility of ratios determined from at least three aliquots of the same samples were within the uncertainties calculated for a single sample (average relative uncertainty of 0.0020 % for $^{206}Pb/^{207}Pb$ and 0.0026% for $^{208}Pb/^{207}Pb$).

2.3 Major and trace element analyses

For each digestion run, twelve sediment samples of approximately 0.09 g to 0.1 g were weighed directly into 90 mL-TFM microwave tubes (MLS GmbH, Leutkirch, Germany). Each sample was digested using 1,5 mL 65 % HNO3 (subboiled twice, Roth ROTIPURAN® p.a., Carl Roth GmbH + Co. KG, Karlsruhe, Germany), 1mL 48 % HF (Roth ROTIPURAN® Supra), and 0,5 mL 34 % HCl (Roth ROTIPURAN® Ultra) in a ETHOS.lab microwave system (MLS GmbH, Leutkirch, Germany). After cooling down, the solutions were evaporated to complete dryness and 15 mL (3x5 mL) of 1 % HNO3 (subboiled twice, Roth ROTIPURAN® p.a.) were added to the residues.

https://doi.org/10.5194/egusphere-2026-3608
Preprint. Discussion started: 30 June 2026

Trace element analyses (Pb, Mn, Ni, Co, Zn, Zr, Cr) were conducted using an 8900 ICP-MS Triple Quadrupole (Agilent Technologies). For quality control, triple measurements, blanks, standards and certified reference materials (IAEA 456 Marine Sediment standard material) were analyzed at frequent intervals. Certified values for all elements and the results of repeated measurements can be found in Table S6, SI. All measured concentrations were corrected by subtracting blank values and exclusion of measurements with concentrations below the limit of quantification (LOQ).

Iron (Fe) and calcium (Ca) concentrations in the digested samples were determined using inductively couple plasma – optic emission spectrometry (ICP-OES/Varian ES715). For quality control, triple measurements, and the measurements of standards and the certified reference material (IAEA 456 Marine Sediment) were conducted. All measured concentrations were corrected via subtraction of the blank and exclusion of values with concentrations below the LOQ. Triplicate measurements (n = 6) were used to calculate the relative standard error of the mean, which was between 1.5 and 6.5 % for all measured elements.

Concentrations of (Si, Al, K, Mg, P, Na, Ti, Rb, Ba and Sr) in sediments were determined by means of wavelength dispersive X-ray fluorescence spectroscopy (WD-XRF; ZSX Primus II, Rigaku, Tokyo, Japan) at Institute of Landscape Ecology, Ecohydrology and Biogeochemistry Group, University of Münster. To this end, 500 mg of powdered sample were pressed to a 13 mm pellet under vacuum and a load of 7 to, adding 50 mg of Hoechst Wax (Sigma Aldrich Merck KGaA, Darmstadt, Germany) as pelleting aid. The instrument was calibrated with a set of 15-20 reference materials in a similar form of pellets (depending on the respective element), and regularly checked for drift using a working standard.

2.4 CNS Analysis

Total Carbon (TC) concentrations in the solid samples were determined using an Element-analyser Euro EA 3000 by HEKAtec. Calibration was performed using certified BBOT and sulfanilamide standards. For total organic carbon (TOC) analysis, inorganic carbon was removed by pre-treating the samples with 2 mol L^{-1} HCl (Ryba and Burgess, 2002). Reference materials were measured regularly for quality control, the results of which are given in Table S7, SI. Triple measurements ($n = 5$) were conducted in intervals

https://doi.org/10.5194/egusphere-2026-3608
Preprint. Discussion started: 30 June 2026

of eight samples. From these, the relative standard error of the mean was calculated (0.4 – 3.2 % for all measurements).

2.5 Excess ^{210}Pb analysis and calculation of mass accumulation rates

Excess ^{210}Pb ($^{210}Pb_{ex}$; half-life of 22.3 y) concentrations in the sediment samples (Table S8, SI) were measured using two gamma-ray spectrometry systems. Sediment samples were dried and homogenized using an agate mortar. Two grams of sediment were hermetically sealed in plastic tubes and stored for more than two months to establish secular equilibrium between ^{226}Ra and ^{222}Rn.

The peak areas of ^{210}Pb (46.5 keV) and ^{214}Pb (351.9 keV) were measured using GWL120230 and GWL120-15 (both AMETEK ORTEC, Oak Ridge, USA) well-type high-purity germanium detectors. Sample counting times ranged from 1 to 3 days. These peak areas were determined by Gaussian curve fitting using KaleidaGraph (Synergy Software, Minneapolis, USA). Concentrations of ^{210}Pb and ^{214}Pb were quantified by comparison with peak areas obtained from the reference material DL-1a (Canada Centre for Mineral and Energy Technology, Ottawa, Canada). The $^{210}Pb_{ex}$ concentration was calculated by subtracting the ^{214}Pb concentration from the total ^{210}Pb concentration, assuming secular equilibrium between ^{226}Ra and ^{222}Rn in the sediment. In case two-standard deviations of the mean $^{210}Pb_{ex}$ reached negative values, the data was removed from the dataset to be considered below background level.

Mass accumulation rates of the respective cores were calculated from $^{210}Pb_{ex}$ profiles showing mono-exponential declines and from cumulative mass derived from dry bulk density and thickness of each sediment section, based on the Constant Flux-Constant Sedimentation (CF:CS) model (Krishnaswamy et al., 1971; Oguri et al., 2022).

2.6 Statistical analysis

The statistical analysis was performed using Microsoft Excel 2019 including the XLMiner Analysis ToolPak as well as RStudio 2023.03.0-daily+82.pro2 (R Core Team 2020). In order to determine correlation coefficients and *p*-values, due to the small sample size (n = 17 per station) and the presence of non-normally distributed variables (Shapiro-Wilk test, $p < 0.05$), Spearman rank correlation was used. Plots were created using the GGplot2 package in R and OriginPro2026.

https://doi.org/10.5194/egusphere-2026-3608
Preprint. Discussion started: 30 June 2026

3 Results & Discussion

3.1 Study Area & Sedimentary setting

The study area in the Scotia Sea is known for its high primary productivity (El-Sayed, 1988; Soppa et al., 2016; Borrione and Schlitzer, 2013), leading to large quantities of biogenic particles including diatom detritus being transported to the sediments (Klaas, 2022). Although some anthropogenic Pb inputs have been identified in the SAO, water phase Pb pollution remains relatively small (16.7 ± 3.8 pmol kg^{-1} in the western South Atlantic (Olivelli et al., 2023)), in parts even approaching near natural conditions (Howe et al., 2004; Noble et al., 2012), enabling the exploration of natural Pb isotope distributions. Deep sea sediment cores, with a length of 26.3, 12.5 and 13.5 cm, were extracted from three sampling stations located in vicinity to South Georgia (PS133/1_9-22; St9), within (PS133/1_15-5; St15) and next (PS133/1_16-1; St16) to the South Sandwich Trench (Fig. 1) during the Polarstern expedition PS133/1 at 3795.8 m below sea level (mbsl), 8066.4 mbsl and 5002.1 mbsl, respectively. Pictures taken directly after sampling can be found in supplementary information (SI), Fig. S1.

The chemical sediment composition is crucial for understanding the relationship between Pb sedimentation, productivity and mineral particle accumulation. Our approach of investigating sediment cores as a function of water depth assumes that biogenic silicon and organic carbon are continuously dissolved and lost from particulate matter during sinking as a result of increasing pressure, decreasing temperature and organic matter mineralization (Omand et al., 2020; Stief et al., 2023). Accordingly, we assumed that the sediment core taken from the deepest station (St15) reflects the most degraded and altered particulate matter composition.

An overview of sedimentary settings can be found in Table S1 alongside boxplots displaying relevant sediment constituents in Fig. S2 and S3. The sediment at St15 (Meteor Deep) exhibited the lowest silicon content (20.6 – 26.4 %), with an average of 23.0 %, significantly lower (p-value < 0.001, Kruskal-Wallis Test) than at St9 (31.2 % on average) (Fig. S2, SI). Similarly, TOC contents (~ 0.32 %) at St15 were less than half of those found at St9 (~ 0.77 %) and lower concentrations of organic pigments were measured

https://doi.org/10.5194/egusphere-2026-3608
Preprint. Discussion started: 30 June 2026

in the first centimeter of the sediment core (chlorophyll-a ~ 28 ng ml^{-1}, Table S1, SI), indicating lower biogenic input.

At St15, Pb concentrations varied from 2.9 to 11.6 µg g^{-1} (mean 7 µg g^{-1}) and were the highest of all three cores, similar to Al concentrations (~ 40 mg g^{-1}) indicating relatively high lithogenic input (Fig. S2, SI). Moreover, the relatively low Si- and TOC- as well as the high Pb concentrations (Fig. S2, SI), indicated Si and C losses and Pb enrichment during sinking through the water column. The positive correlation of Pb concentrations with TOC contents (Fig. 3) suggests that the sedimentation of Pb is largely controlled by that of organic matter, which is in line with its affinity to absorb onto organic particles (Chuang et al., 2014). Compared to Si concentrations, Pb and TOC concentration patterns showed an offset of about 1 cm (Fig. 3), probably due to the faster sinking speed of biogenic silicon compared to organic carbon, which appears to be pronounced at such large depth (Tréguer et al., 2021; DeMaster et al., 1992; Pichevin et al., 2014; Griffiths et al., 2026), or due to a density separation during sedimentation.

St16 showed silicon contents between 23.3 – 33.4 %, lower than at St9, but exceeding those at St15 (Fig. S2, SI). Similarly, organic carbon contents (~ 0.5 %) were roughly two thirds compared to sediments at St9 and chlorophyll-a concentrations in the upper centimeter (~18 ng ml^{-1}) were significantly lower than at St9, indicating lower inputs of OM and diatom remains. Downcore Pb concentrations (4.3 to 7 µg g^{-1}, mean 6 µg g^{-1}) at St16 were similar to those at St9, but showed higher median concentrations of 6.2 µg g^{-1} compared to 4.8 µg g^{-1} suggesting higher dilution by diatom remains at St9 as indicated by the high Si content. The same applied to Al concentrations at St 16 (~ 16.5 mg g^{-1}) (Fig. S2, SI). We thus observed a partly inverse picture compared to St15. Si as well as TOC concentrations were higher, but Pb concentrations, like other lithogenic elements, were lower compared to St15 (Fig. S2 – S3, SI). This was probably due to the shallower depth (~5000 m) and therefore lower pressure- and less dissolution of biogenic silica at St 16 and St9. Thus, the higher Si concentrations, which dominated the composition of the sediments, diluted the concentrations of all other major and trace elements.

The sediment at St9 consisted mainly of diatom-ooze, with silicon concentrations from 29 – 33 % (Fig. S2, SI), indicating intense diatom-blooms in the surface waters and high Si export to the sediment. High

https://doi.org/10.5194/egusphere-2026-3608
Preprint. Discussion started: 30 June 2026

organic matter input at this station was further indicated by comparatively high organic carbon contents (~ 0.77 %) and chlorophyll-a concentrations (431 ng ml^{-1}) in the upper centimeter. Pb concentrations varied from 4.1 to 7.2 µg g^{-1} (mean 5 µg g^{-1}) while Al showed a mean concentration of 17 mg g^{-1}, both significantly lower than in the other cores (Fig. S2, SI).

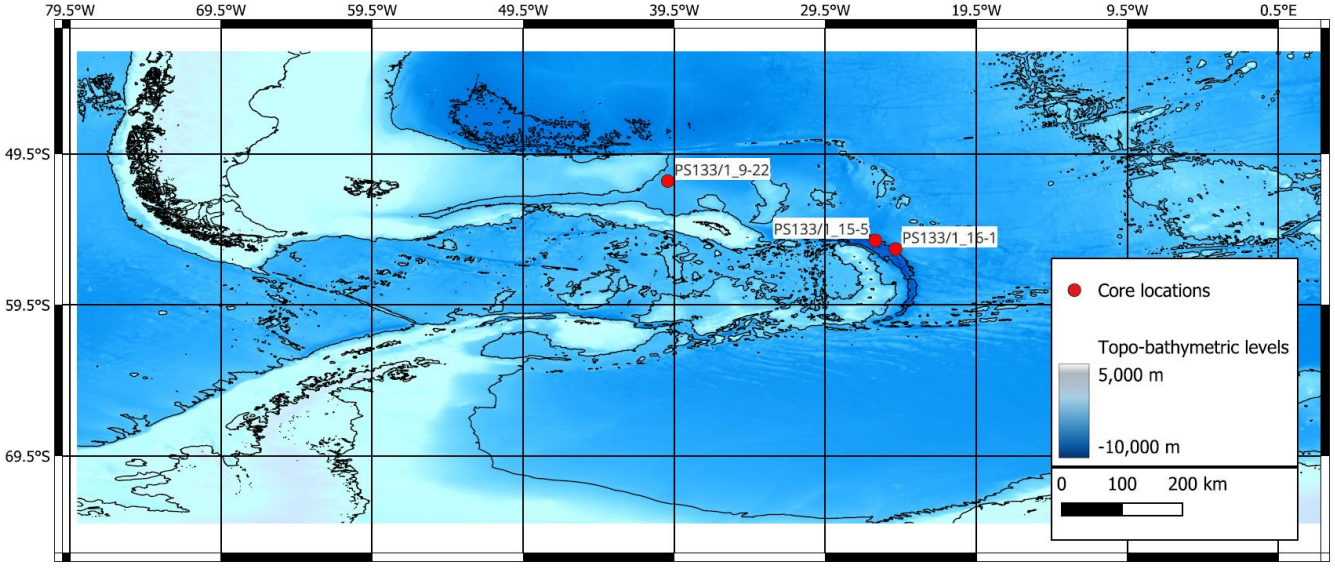

Figure 1: Bathymetry and topography map of the sampling sites PS133/1_9-22 (St9), PS133/1_15-5 (St15) and PS133/1_16-1 (St16) at the South Sandwich Trench based on gridded data (15 arc-second intervals) obtained from the General Bathymetric Chart of the Oceans (GEBCO www.gebco.net) using the current gridded global terrain dataset GEBCO_2024.

Besides anthropogenic Pb sources, atmospheric deposition of natural dust is the major source of Pb to the open ocean (Bridgestock et al., 2016; Olivelli et al., 2025). The transport of dissolved anthropogenic and natural Pb to the SAO by ocean currents has been suggested in previous Pb isotope studies (Olivelli et al., 2025; Olivelli et al., 2023), but has not yet been confirmed by sediment records. A three-isotope plot of the Pb isotope ratios measured in the three sediment cores (Fig. 2) reveals that apart from minor variation, the measured Pb isotope ratios at the different stations all overlapped within a small range, suggesting the same Pb source. The overall isotope signatures were uniform, with ratios ranging between

https://doi.org/10.5194/egusphere-2026-3608
Preprint. Discussion started: 30 June 2026

1.195 and 1.212 for $^{206}Pb/^{207}Pb$ (1.203 ± 0.003, n = 44) and 2.475 - 2.489 for $^{208}Pb/^{207}Pb$ (2.484 ± 0.003, n = 44) (Fig. 2).

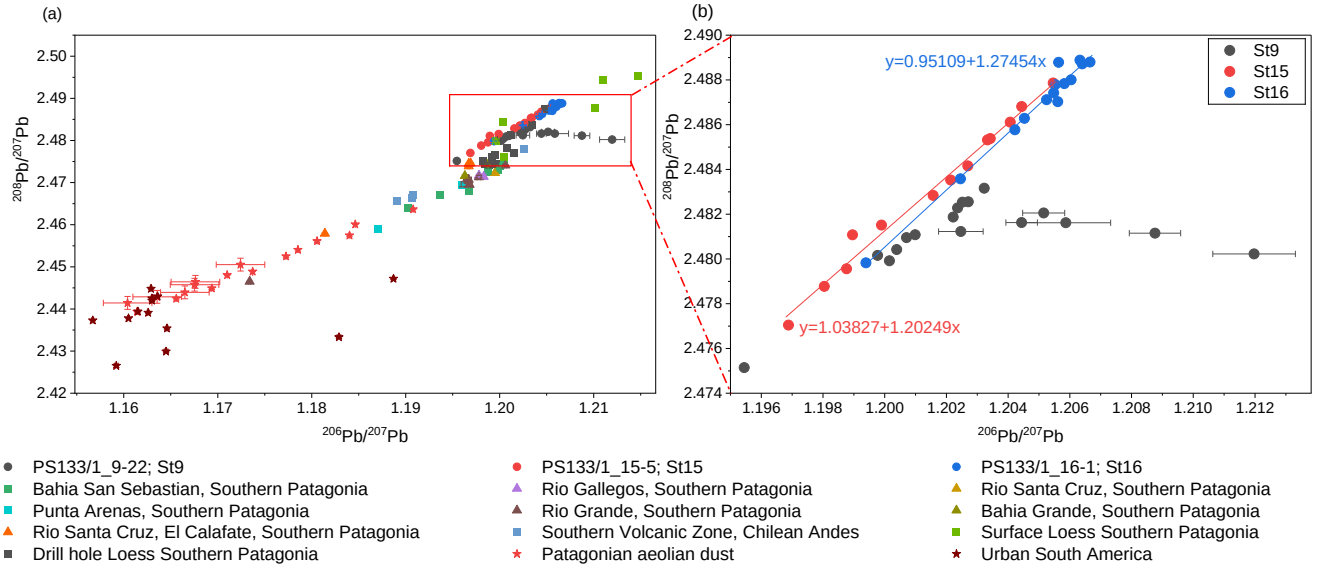

Figure 2: a. Pb isotope fingerprints of top-soils (squares), river sediments (triangles), dust and aerosols (stars) from Southern Patagonia (compiled from (Khondoker et al., 2018; Gili et al., 2016)) in relation to measured Pb isotopes from this study. b. Close up three-isotope plot of $^{206}Pb/^{207}Pb$ plotted against $^{208}Pb/^{207}Pb$ from St9, St15 and St16. Error bars are included, but are in some cases smaller than the symbols.

The range of Pb isotope ratios was compared to the isotope fingerprint of top-soils, river sediments, dust and aerosols from Southern Patagonia (Khondoker et al., 2018; Gili et al., 2016; Olivelli et al., 2023). All Pb isotope ratios of the examined sediments fell within the natural Patagonian isotope fingerprint (Fig. 2), revealing Patagonian natural dust as the main Pb source for sediments in this part of the SAO. The predominance of natural, lithogenic Patagonian Pb is due to the overwhelming presence of strong westerly winds between 40 and 50° latitude in the Southern Hemisphere (Bracegirdle, Thomas J. & National Center for Atmospheric Research Staff), transporting dust towards the SAO and introducing it to the ocean water via wet and dry deposition (Weis et al., 2024). From Fig. 2 it becomes evident, that anthropogenic sources played none or an only very minor role for the Pb isotope signature in the sampled sediments, a finding which deviates from what has been reported for dissolved Pb in the water column (Schlosser et al., 2019).

https://doi.org/10.5194/egusphere-2026-3608
Preprint. Discussion started: 30 June 2026

3.2 Pb Isotope variability in the sediments at depth

With a single Pb source, one would expect little or no variation in the Pb isotopic signatures in the sediments, with the average representing mostly the initial source signal (Komárek et al., 2008; Cullen and McAlister, 2017). However, Pb isotope ratios showed clear variability within all three sediment cores (Figs. 3-5), while remaining within the confines of the identified Patagonian source signal. Accordingly, the observed changes could reflect Pb isotope fractionation processes during sediment diagenesis and associated changes in redox conditions (Deng et al., 2022), selective scavenging of phase Pb from different water masses (Chuang et al., 2014), or changes in exported suspended particle-bound Pb isotopes as a result of reverse scavenging processes (Bridgestock, 2023; Lanning et al., 2023; Olivelli et al., 2024; Bacon et al., 1976). We assume that Pb isotope fractionation does not occur within sediments and that Pb mobility related to redox zonation plays only a minor role (Tsunogai et al., 1979), as no clear relationships between depth profiles of Fe and Mn concentrations and $^{206}Pb/^{207}Pb$ ratios were discernable (Fig. S5 – S7, SI). Pb isotope fractionation could occur during transformation of Pb binding forms in the sediments, such as the formation of PbS during OM mineralization under sulphate reducing conditions (Tsunogai et al., 1979). However, to see such effects in the distribution of Pb isotopes, a considerable amount of Pb must be removed from the sediment. Previous studies have shown that Pb isotope signatures in sediments remain largely stable, with only minor influence of pore water fluxes or resuspension, which do not occur at large water depths (Zhao et al., 2013; Erhardt et al., 2021; Hamelin et al., 1990; Homoky et al., 2016). To decipher the relationship between particulate matter loads as an indicator of changes in productivity and Pb concentrations and isotope signatures in sediments, we compared them with sediment silicon and total organic carbon content (Figs. 4-6). The use of silicon as an indicator of primary production by diatoms assumes that the dominant source in these diatom-ooze dominated sediments is biogenic and that mineral quartz particles are less prevalent. Moreover, we assume that other primary producers such as coccolithophores or pteropods ($CaCO_3$ sources) are relatively minor contributors. In addition, we used Pb/Al ratios to distinguish TOC associated from mineral particulate matter associated Pb fractions (Fig. S10, SI). Assuming that Pb isotope signatures are stable in sediments, correlations with Si and C in an area defined by a single Pb source would suggest Pb isotope exchange processes along the water column.

https://doi.org/10.5194/egusphere-2026-3608
Preprint. Discussion started: 30 June 2026

Pb isotope ratios $^{206}Pb/^{207}Pb$ and $^{208}Pb/^{207}Pb$ at St15 showed a positive correlation to total Pb and TOC concentrations (Fig. 3), which suggests that the intensity of productivity at the surface ocean influences the Pb isotope signature of these sediments. The effect of biogenic particulate matter on dissolved and dust phase Pb isotopes is yet not exactly known. As reported by Schlosser et al. (2019), biogenic particles may adsorb dissolved Pb from the water phase during phytoplankton blooms. In addition, it is known that biogenic particulate matter and mineral dust form aggregates which contain formerly dissolved Pb bound to organic matter, and the mineral dust phase (Barkmann et al., 2010; Ren et al., 2023). During these processes, a separation of Pb isotope pools related to their solubility and particle-reactiveness could occur (Griffiths et al., 2026), leading to the formation of Pb pools with different isotope fingerprints similar to what has been observed in river beds (Izquierdo et al., 2012). We hypothesize that during sinking, due to progressive decomposition and carbon loss, the particulate matter aggregates are likely re-accumulating the previously dissolved Pb fraction in organic matter, causing for a characteristic Pb isotope fingerprint. In addition, some mineral-associated Pb phases are likely being dissolved with increasing depth due to pressure effects or redox induced dissolution of Fe/Mn phases, while low-solubility phases remain unchanged during vertical transport, preserving their original (dust) Pb isotope fingerprint (Harlavan and Erel, 2002).

https://doi.org/10.5194/egusphere-2026-3608
Preprint. Discussion started: 30 June 2026

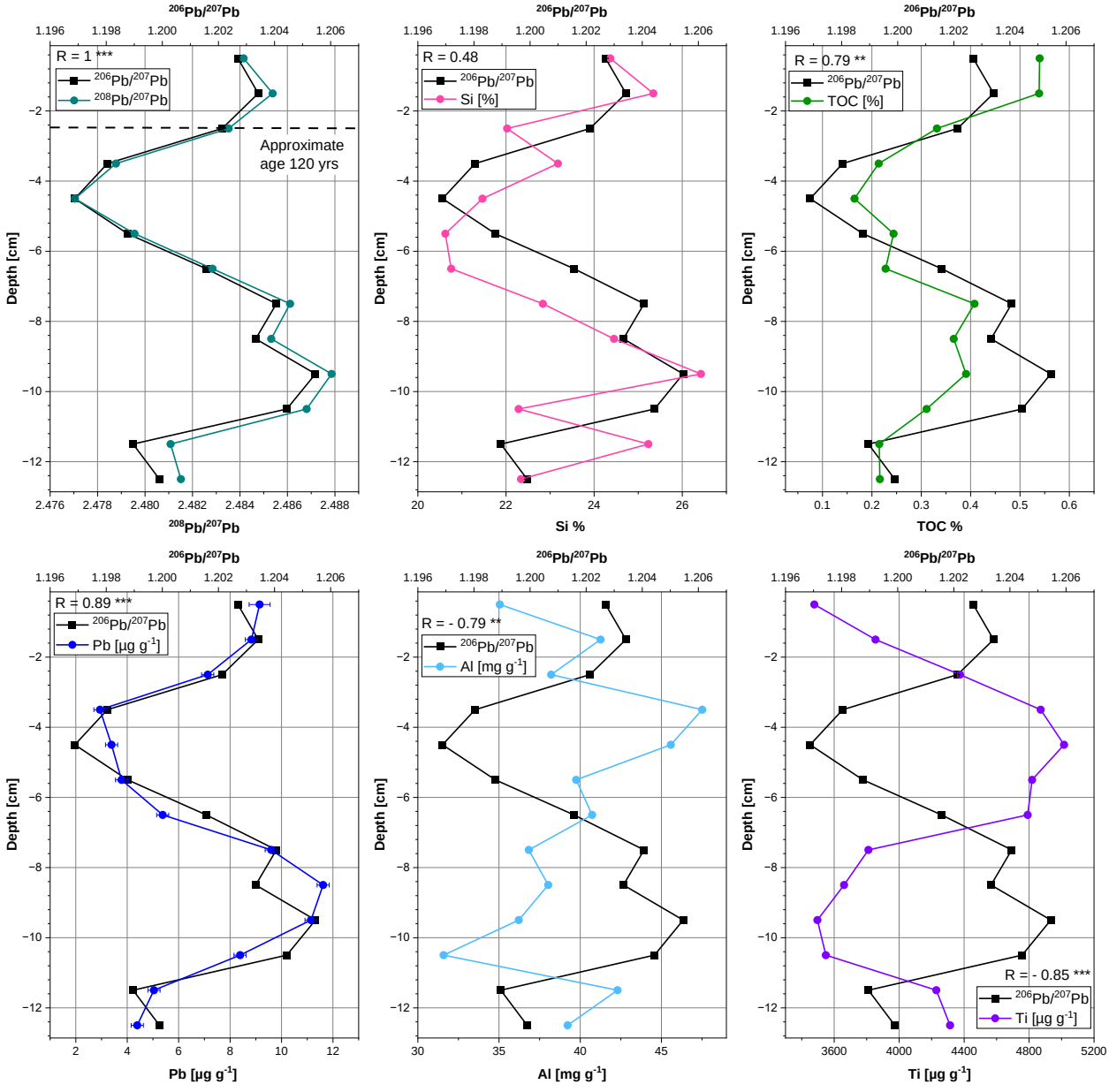

Figure 3: Depth profiles of the $^{206}Pb/^{207}Pb$ & $^{208}Pb/^{207}Pb$ ratios and Si, TOC, Pb, Al and Ti concentrations in the sediment core from St15. Error bars are included but are in some cases smaller than the symbols.

The increase in all Pb isotope ratios with higher productivity could reflect interactions between mineral particles, Pb dissolution and Pb scavenging by organic matter in the water column (Winter et al., 1997).

https://doi.org/10.5194/egusphere-2026-3608
Preprint. Discussion started: 30 June 2026

The initial process may involve preferential dissolution of labile Pb phases from dust in the water phase (Maccali et al., 2012; Harlavan and Erel, 2002), leaving the residual mineral (dust) particles with distinct $^{206}Pb/^{207}Pb$ and $^{208}Pb/^{207}Pb$ ratios. Under relatively low productivity conditions (low TOC concentrations) organic matter preferentially adsorbs this dissolved Pb fraction so that their Pb isotopic signal is transferred to the biogenic particulate matter, while a different isotopic signal will be retained in mineral particles. During low productivity conditions, the aggregation of mineral particles, containing the mineral particle specific Pb isotopic signature with biogenic particles is then lower. With increasing productivity, higher amounts of particulate matter are likely to enhance aggregation with mineral particles (ballasting), resulting in different Pb isotope ratios in the sediments. Moreover, with increasing water column depth and pressure as well as microbial activity on particles and increased sinking time, Pb bearing minerals (e.g. Fe/Mn-oxides and biogenic silicon) are progressively dissolved, and the released trace elements are re-scavenged by organic matter (Comstock et al., 2024; Griffiths et al., 2026). This process would also explain why other metals such as Ni, Cr and K were also significantly correlated with TOC in this core (Fig. S13, SI). However, other lithogenic metals such as Al, Cu, Ti, and Zr were negatively correlated with TOC (Fig. 3 and correlation matrix Fig. S13, SI), indicating that those stables phases (e.g. quartz, clay minerals) are not dissolved. This was supported by the relatively high Al concentrations at St15 compared to the sediments of the other stations (Fig. S2, SI). The negative correlation of the Pb concentrations (and Pb isotopes ratios) with Al, Cu, Ti, and Zr concentrations suggest that Pb had been largely removed from those altered mineral particles during sinking. Assuming that nearly all Pb had been dissolved during sinking and subsequently scavenged by organic matter, the amount of TOC appeared to control the isotope composition of Pb in the settling biogenic particles (Chuang et al., 2014). Low amounts of organic matter will mainly adsorb Pb isotopes from the dissolved phase, as it has been observed for Ni and Cd (Archer et al., 2020; Ripperger et al., 2007), while with increasing amounts of organic matter (higher productivity) and Pb binding sites, progressively more Pb – including mineral' particle associated Pb isotope signatures – are scavenged, increasing the overall variability of all Pb isotope ratios.

Pb isotope ratios at St 16 showed less variability than at St15, but a pronounced significant correlation with Si ($R = 0.83$, $p < 0.001$) (Fig. 4). Different from St15, Pb isotope ratios were negatively correlated

https://doi.org/10.5194/egusphere-2026-3608
Preprint. Discussion started: 30 June 2026

with TOC (R = - 0.57, p = 0.032, Table S2, SI), indicating decreasing Pb isotope ratios with increasing TOC content. Moreover, unlike St15, Pb concentrations at St16 were only weakly correlated with carbon and Si but positively correlated with most lithogenic elements (Al, K, Cu, Zn, Co, Ti, Zr) (Fig. S14, SI), suggesting that a larger fraction of mineral phase Pb was preserved. Si also showed a strong correlation with Al, Fe and most lithogenic elements, which indicated that Si was partly lithogenic (quartz) and/or that particles were apparently deposited together with biogenic opal and TOC as aggregates.

The decrease of Pb isotope ratios in the upper 6 cm of the core (Fig. 4) may reflect water phase downward transport of anthropogenic Pb from the surface via sinking particles, as shown by water-phase data from other studies (Lanning et al., 2023; Olivelli et al., 2024). Alternatively, the decrease of both isotope ratios may indicate preferential dissolution of a relatively labile mineral phase in the upper ocean with a distinct isotope signature (Harlavan and Erel, 2002; Dausmann et al., 2019; Izquierdo et al., 2012). The dissolution of mineral phases containing Pb is likely a function of water depth and related increasing pressure as well as dissolution of Pb bearing redox sensitive Fe/Mn phases, resulting in depth-dependent release of Pb from different minerals. The negative correlation between Pb isotope ratios and TOC suggests that the dissolved Pb from those labile mineral Pb phases is preferentially bound to organic matter, whereas Pb with characteristic isotope ratios is still bound in the mineral phase.

At both, St15 and St16, Pb isotopes ratios correlate positively with Si (Figs. 3-4), indicating that changes in sedimentation of Pb at both sites are driven by productivity. A key difference is that in sediments at St16, most Pb appears to be still bound in mineral particles (no correlation with TOC), whereas at St15, most mineral Pb phases were apparently dissolved and subsequently associated with organic matter.

https://doi.org/10.5194/egusphere-2026-3608
Preprint. Discussion started: 30 June 2026

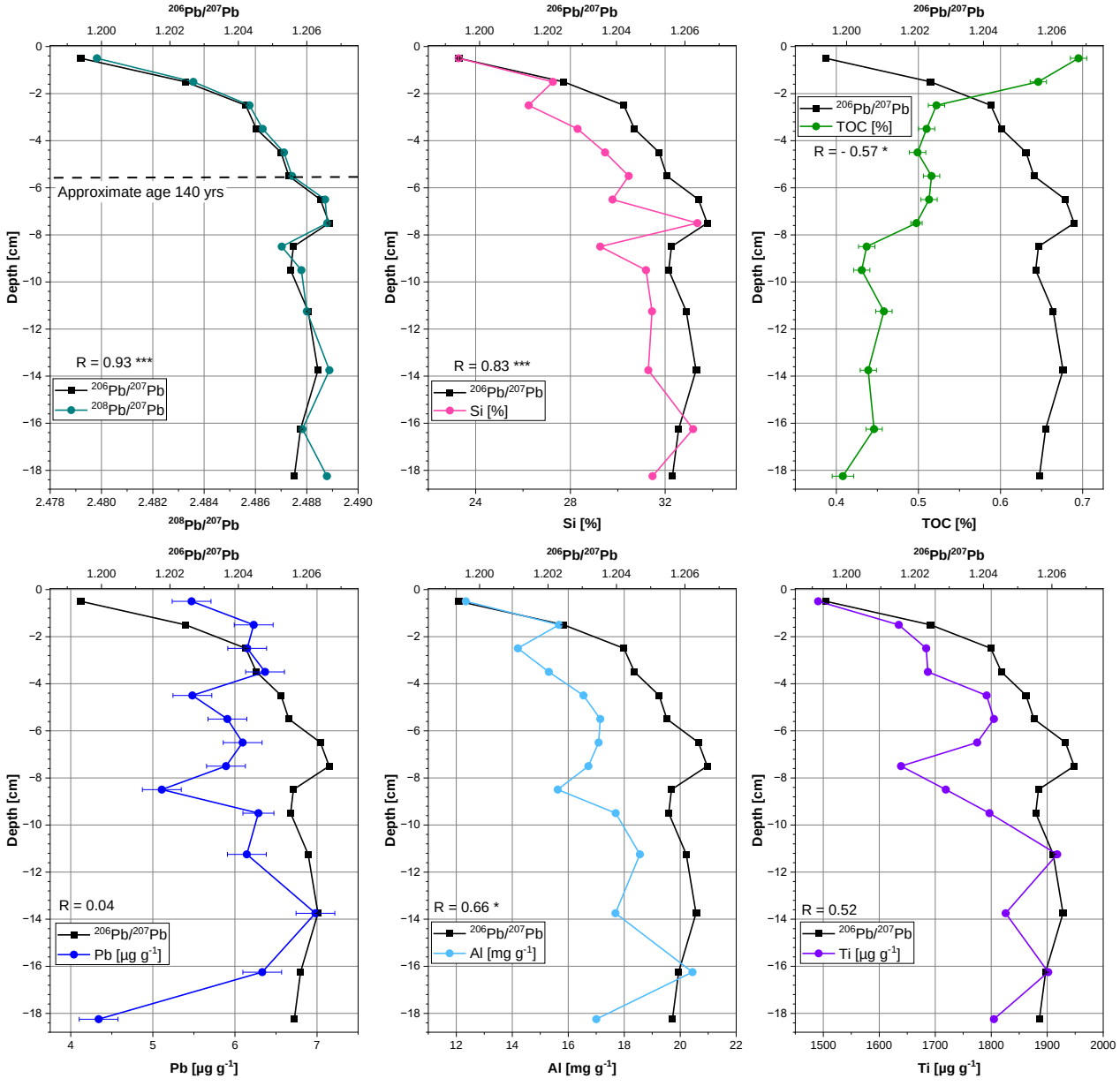

Figure 4: Depth profiles of the $^{206}Pb/^{207}Pb$ & $^{208}Pb/^{207}Pb$ ratios plotted alongside Si, TOC, Pb, Al and Ti contents in the sediment core from St16. Error bars are included but are in some cases smaller than the symbols.

https://doi.org/10.5194/egusphere-2026-3608
Preprint. Discussion started: 30 June 2026

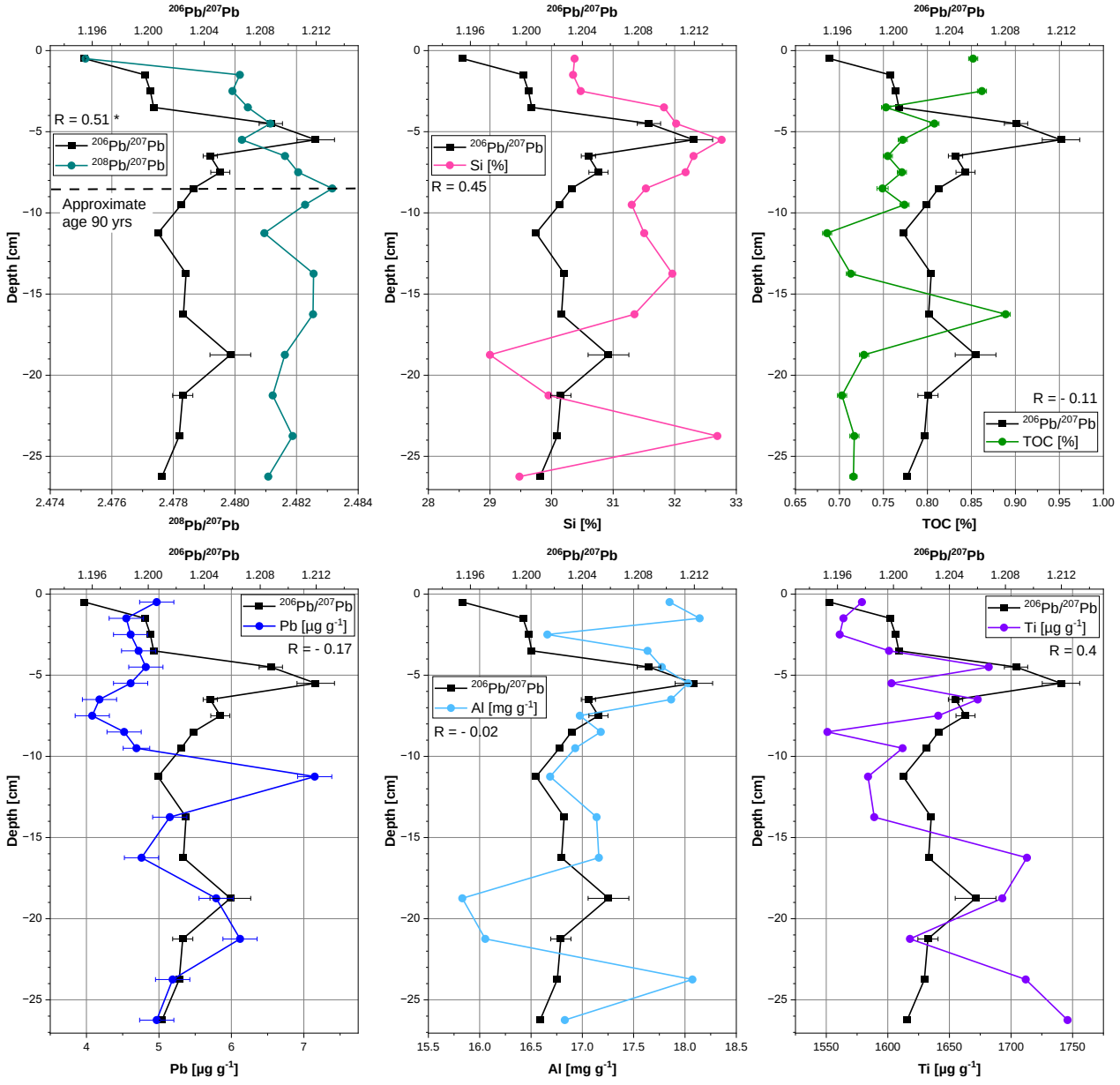

Figure 5: Depth profiles of the $^{206}Pb/^{207}Pb$ & $^{208}Pb/^{207}Pb$ ratios plot against Si, TOC, Pb, Al and Ti contents in the sediment core from St9. Error bars are included but are in some cases smaller than the symbols.

https://doi.org/10.5194/egusphere-2026-3608
Preprint. Discussion started: 30 June 2026

St9 showed a much less clear relationship between Pb concentrations, Pb isotopes and the productivity proxies Si and TOC. The most important difference to the cores from the other stations was that, despite sediment accumulation at a constant rate and no evidence of bioturbation or sediment re-working, the downward trends of the isotope pairs $^{206}Pb/^{207}Pb$ and $^{208}Pb/^{207}Pb$ were not correlated, as it was observed at the other stations (Fig. 5). This implies that the distribution of Pb isotope pools was not only determined by dissolution of particles from a single dust source and subsequent scavenging processes, but also by a second Pb source, particularly dominant around 5 and 20 cm sediment depth. This interpretation is further supported by the higher accumulation rates of Pb in the sediment at St9 (0.12 mg Pb m^{-2} yr^{-1} vs 0.09 and 0.07 mg Pb m^{-2} yr^{-1} at St 15 and St 16 respectively; calculated from $^{210}Pb_{ex}$ profiles, Fig. S11, SI).
St9 is about 1200 km west of St15 and is therefore closer to the Patagonian shelf, which might explain the influence of an additional Pb source through dust or current patterns, although the sedimentary isotope signature remained within the range of Patagonian dust. The influence of another Pb source, characterized by larger ratios of $^{206}Pb/^{207}Pb$, was also evident from the three-isotope plot which clearly deviated from that of the other stations (Fig. 2). Although the correlation of the Pb isotope pairs ($^{206}Pb/^{207}Pb$ and $^{208}Pb/^{207}Pb$) and other sediment constituents were only weak (Fig. S15, SI), some parts of the core showed good agreement with Pb isotope ratios, especially the ratio $^{206}Pb/^{207}Pb$, and Al (Fig. 5), which suggested influence of lithogenic rather than biogenic particulate matter. This particle source could be a nepheloid layer formed by material resuspended from the Patagonian shelf through currents, a material which appears to show the largest $^{206}Pb/^{207}Pb$ ratios. Similar patterns have been reported for dissolved Pb isotopes in the South Atlantic (Olivelli et al., 2024).

Silicon concentrations at St9 correlated only weakly with Pb isotope ratios ($R = 0.45$, $p = 0.068$, Fig. 5) and almost no correlation was observed between Pb concentrations and Pb isotope ratios, which we mainly attribute to the high dilution of Pb concentrations by biogenic silicon at this site. The correlation of Pb concentrations with TOC was slightly negative, again attributed to the dilution effect of the relatively high TOC concentrations at St9. We did, however, observe a negative correlation of Pb with Al and Ti (Fig. S15, SI), which may indicate that considerable parts of Pb are associated with TOC. Moreover, in discrete sections of the core Pb isotope ratios followed the course of TOC, Si or Pb

https://doi.org/10.5194/egusphere-2026-3608
Preprint. Discussion started: 30 June 2026

concentrations (Fig. 6). This suggests that similar processes of the separation of different Pb isotope pools (in the water column) connected to particle dissolution and scavenging as described for the other cores occur, but are blurred by the high sedimentation rates (0.95 mm yr^{-1} vs 0.21 and 0.4 mm yr^{-1} at St15 and 16, respectively (Table S1, SI)).

Overall, the observed changes in Pb isotope ratios in all cores appeared to be a result of mixing, dissolution, aggregation and degradation of different particles in the water phase during sinking, with most processes strongly controlled by productivity and the occurrence of organic particles, rather than a result of changes in the Pb source.

In this study, dissolved or suspended Pb isotopes were not measured in the water phase, so that a direct comparison to Pb isotope signatures in the sediments was not possible. A key question in understanding the relationship between dissolved Pb isotopes in the water column and Pb isotope signatures in underlying sediments is to which extent Pb dissolution from dust and reversible scavenging of dissolved Pb by organic particles alter the Pb isotope signature in the water and particulate phases. Olivelli et al (2024) showed that aerosols and their leachates display a similar Pb isotope pattern to the seawater samples along a transect at 40 °S (GEOTRACES Section GA10), about 10 to 15 ° north of our sampling area, indicating dissolution of Pb from local atmospheric dust. Selective dissolution of Pb phases of dust suggest that formation of isotopically different Pb pools between the dissolved and the particulate phase occurs. Assuming that isotope ratios of dissolved Pb in the water column above our sampling sites were similar to those shown by Olivelli et al., 2024, these processes would also explain the consistent offset between Pb isotope ratios in the water phase (Olivelli et al., 2024) and those observed in our sediment cores. While Pb isotopes measured in the water phase exhibit $^{206}Pb/^{207}Pb$ ratios of 1.16 to 1.18 (Olivelli et al., 2023; Olivelli et al., 2024; Olivelli et al., 2025), $^{206}Pb/^{207}Pb$ ratios measured in the sediments range from 1.12 to 1.21. A similar effect of larger isotope ratios in sediments was also found for the ratios of $^{208}Pb/^{207}Pb$ (2.42 – 2.46 in the water phase (Olivelli et al., 2023; Olivelli et al., 2024; Olivelli et al., 2025) and 2.475 – 2.49 in our sediments (Fig. S4, SI)

4 Conclusions

https://doi.org/10.5194/egusphere-2026-3608
Preprint. Discussion started: 30 June 2026

Pb isotope signatures in three pelagic sediment cores from the South Atlantic could clearly be related to Patagonian dust as the dominant Pb source, although one of the cores exhibited Pb isotope patterns indicating influence from particles likely derived from the Patagonian shelf. Despite a single, common Pb source, Pb isotope ratios in all sediment cores showed distinct variations. Pb isotope ratios in sediments were consistently larger than those observed for water-phase Pb in previous studies from the same region, indicating a separation and preferential scavenging of different dissolved Pb pools in the water column. Variations in Pb isotope ratios in the sediment were found to be related to the content of biogenic silicon and organic carbon, indicating a strong influence of primary productivity and biogenic particles on Pb scavenging in the mixed layer and corresponding isotope ratios. This relationship was most pronounced in the sediment core taken at the deepest sampling point (8066 mbsl), where a large proportion of biogenic silicon as well as most mineral Pb phases had apparently been dissolved during vertical transport. This became evident from a strong positive correlation of Pb concentrations and Pb-isotope ratios with Si and TOC, and a negative correlation with Al. This relationship was less pronounced or absent at shallower sites, where TOC and Pb concentrations were diluted by high contents of biogenic silicon or overprinted by a second Pb source.

Our results indicate that Pb isotope ratios in sediments do not mirror those of dissolved Pb in the water phase but are likely a result of a separation of Pb pools characterized by distinct isotope signatures induced by selective scavenging in the water column. Our data supports previous assumptions and findings that dissolved Pb isotope ratios in the water column are influenced by scavenging in particle rich areas related to high productivity and are not solely controlled by the source of different water masses. Consequently, these findings question the use of Pb isotope signatures in deep sea sediments to trace Pb sources or water masses. The interplay between scavenging of Pb in the water phase, the dissolution of Pb mineral phases and biogenic opal as well as the mineralization of organic matter of sinking particles with increasing water depth needs further investigation to better constrain how Pb isotopes signatures are altered during particle descend and ultimately preserved in deep sea sediments, particularly in highly oceanic productive regions.

https://doi.org/10.5194/egusphere-2026-3608
Preprint. Discussion started: 30 June 2026

Supplement link

The link to the supplement will be included by Copernicus, if applicable.

Author contributions

Conceptualization: H. Biester, M. Pérez-Rodríguez.

Formal analysis: L. Oskamp, H. Biester

Funding acquisition: H. Biester, F. Wenzhöfer, R. N. Glud

Investigation: L. Oskamp, H. Biester, M. Pérez-Rodríguez, A. Calean, K. Oguri, M. Tsuchiya, F. Wenzhöfer, R. N. Glud

Methodology: L. Oskamp, A. Calean, O. Rienitz, K. Oguri, M. Tsuchiya, K.H. Knorr.

Project administration & Supervision: H. Biester

Resources: H. Biester, R. N. Glud

Visualization: L. Oskamp

Writing – original draft: L. Oskamp, H. Biester

Writing – review & editing: L. Oskamp, H. Biester, M. Pérez-Rodriguez, A. Calean, O. Rienitz, K-H. Knorr, K. Oguri, M. Tsuchiya, M. Benkhettab Sindlev, S. Krisch, A. Olivelli, F. Wenzhöfer, R. N. Glud

Competing interests

The authors declare no competing interests relevant to this study.

https://doi.org/10.5194/egusphere-2026-3608
Preprint. Discussion started: 30 June 2026

Acknowledgements

We would like to thank the captain and the crew of RV Polarstern for their support and tireless efforts during research cruise PS133.1, as they faced the challenges of the Southern Ocean. Cruise PS133.1 was dedicated to the projects “Island Impact: Understanding the Regional Impact of South Georgia on Southern ACC Biogeochemistry and Ecosystem Function” and “South Polar Carbon: Benthic Carbon Mineralization and Preservation in Southern Ocean Bathyal, Abyssal and Hadal Sediments.” Ship time was provided under Grants GPF 20-1_053 and GPF 20-2_024. This study was supported by the German Science Foundation (DFG) by a Grant to H.B. (BI 734/23-1) and by the Danish National Research Foundation through the Danish Center for Hadal Research, HADAL (Grant DNRF145). We thank C. Klaas and S. Kasten for the invitation to participate in this expedition, and all scientific cruise participants for their assistance with sample collection. In particular, to the Hadal Biogeochemistry group on board: A. Glud (University of Southern Denmark) and A. Nordhausen (Max Planck Institute for Marine Microbiology). We would like to thank H. Matsuda (JAMSTEC) who exchanged the samples and W. Xiao (HADAL, SDU) for providing NPP data for the region. Finally, we thank P. Schmidt and A. C. Quisobori Cantor (both TU Braunschweig) for their invaluable assistance with sediment samples pre-processing and analyses, and D. Brüggemann and S. Peetz (both University of Münster) for conducting the XRF analyses.

Review statement

The review statement will be added by Copernicus Publications listing the handling editor as well as all contributing referees according to their status anonymous or identified.

https://doi.org/10.5194/egusphere-2026-3608
Preprint. Discussion started: 30 June 2026

References

Archer, C., Vance, D., Milne, A., and Lohan, M. C.: The oceanic biogeochemistry of nickel and its isotopes: New data from the South Atlantic and the Southern Ocean biogeochemical divide, Earth and Planetary Science Letters, 535, 116118, https://doi.org/10.1016/j.epsl.2020.116118, 2020.

Bacon, M. P., Spencer, D. W., and Brewer, P. G.: 210Pb/226Ra and 210Po/210Pb disequilibria in seawater and suspended particulate matter, Earth and Planetary Science Letters, 32, 277–296, https://doi.org/10.1016/0012-821X(76)90068-6, 1976.

Barkmann, W., Schäfer-Neth, C., and Balzer, W.: Modelling aggregate formation and sedimentation of organic and mineral particles, Journal of Marine Systems, 82, 81–95, https://doi.org/10.1016/j.jmarsys.2010.02.009, 2010.

Borrione, I. and Schlitzer, R.: Distribution and recurrence of phytoplankton blooms around South Georgia, Southern Ocean, Biogeosciences, 10, 217–231, https://doi.org/10.5194/bg-10-217-2013, 2013.

Boskabady, M., Marefati, N., Farkhondeh, T., Shakeri, F., Farshbaf, A., and Boskabady, M. H.: The effect of environmental lead exposure on human health and the contribution of inflammatory mechanisms, a review, Environment international, 120, 404–420, https://doi.org/10.1016/j.envint.2018.08.013, 2018.

Boyle, E., Lee, J.-M., Echegoyen, Y., Noble, A., Moos, S., Carrasco, G., Zhao, N., Kayser, R., Zhang, J., Gamo, T., Obata, H., and Norisuye, K.: Anthropogenic Lead Emissions in the Ocean: The Evolving Global Experiment, oceanog, 27, 69–75, https://doi.org/10.5670/oceanog.2014.10, 2014.

Bracegirdle, Thomas J. & National Center for Atmospheric Research Staff: The Climate Data Guide: Southern Hemisphere westerly jet strength and position.: Last modified 2022-09-09, https://climatedataguide.ucar.edu/climate-data/southern-hemisphere-westerly-jet-strength-and-position, last access: 12 August 2024.

Bridgestock, L.: Lead contamination of the deep Pacific Ocean via exchange with sinking particles, Proceedings of the National Academy of Sciences of the United States of America, 120, e2308014120, https://doi.org/10.1073/pnas.2308014120, 2023.

Bridgestock, L., Rehkämper, M., van de Flierdt, T., Paul, M., Milne, A., Lohan, M. C., and Achterberg, E. P.: The distribution of lead concentrations and isotope compositions in the eastern Tropical Atlantic Ocean, Geochimica et Cosmochimica Acta, 225, 36–51, https://doi.org/10.1016/j.gca.2018.01.018, 2018.

Bridgestock, L., van de Flierdt, T., Rehkämper, M., Paul, M., Middag, R., Milne, A., Lohan, M. C., Baker, A. R., Chance, R., Khondoker, R., Strekopytov, S., Humphreys-Williams, E., Achterberg, E. P., Rijkenberg, M. J. A., Gerringa, L. J. A., and Baar, H. J. W. de: Return of naturally sourced Pb to Atlantic surface waters, Nature communications, 7, 12921, https://doi.org/10.1038/ncomms12921, 2016.

Chen, M., Boyle, E. A., Jiang, S., Liu, Q., Zhang, J., Wang, X., and Zhou, K.: Dissolved Lead (Pb) Concentrations and Pb Isotope Ratios Along the East China Sea and Kuroshio Transect—Evidence for Isopycnal Transport and Particle Exchange, J. Geophys. Res., 128, https://doi.org/10.1029/2022JC019423, 2023.

Chen, M., Boyle, E. A., Lee, J.-M., Nurhati, I., Zurbrick, C., Switzer, A. D., and Carrasco, G.: Lead isotope exchange between dissolved and fluvial particulate matter: a laboratory study from the Johor River estuary, Philosophical transactions. Series A, Mathematical, physical, and engineering sciences, 374, https://doi.org/10.1098/rsta.2016.0054, 2016.

https://doi.org/10.5194/egusphere-2026-3608
Preprint. Discussion started: 30 June 2026

Cheng, H. and Hu, Y.: Lead (Pb) isotopic fingerprinting and its applications in lead pollution studies in China: a review, Environmental pollution (Barking, Essex 1987), 158, 1134–1146, https://doi.org/10.1016/j.envpol.2009.12.028, 2010.

Chuang, C.-Y., Santschi, P. H., Jiang, Y., Ho, Y.-F., Quigg, A., Guo, L., Ayranov, M., and Schumann, D.: Important role of biomolecules from diatoms in the scavenging of particle‐reactive radionuclides of thorium, protactinium, lead, polonium, and beryllium in the ocean: A case study with Phaeodactylum tricornutum, Limnology & Oceanography, 59, 1256–1266, https://doi.org/10.4319/lo.2014.59.4.1256, 2014.

Comstock, J., Henderson, L. C., Close, H. G., Liu, S., Vergin, K., Worden, A. Z., Wittmers, F., Halewood, E., Giovannoni, S., and Carlson, C. A.: Marine particle size-fractionation indicates organic matter is processed by differing microbial communities on depth-specific particles, ISME communications, 4, ycae090, https://doi.org/10.1093/ismeco/ycae090, 2024.

Cullen, J. T. and McAlister, J.: Biogeochemistry of Lead. Its Release to the Environment and Chemical Speciation, Metal ions in life sciences, 17, https://doi.org/10.1515/9783110434330-002, 2017.

Dausmann, V., Gutjahr, M., Frank, M., Kouzmanov, K., and Schaltegger, U.: Experimental evidence for mineral-controlled release of radiogenic Nd, Hf and Pb isotopes from granitic rocks during progressive chemical weathering, Chemical Geology, 507, 64–84, https://doi.org/10.1016/j.chemgeo.2018.12.024, 2019.

DeMaster, D., Dunbar, R., Gordon, L., Leventer, A., Morrison, J., Nelson, D., Nittrouer, C., and Smith, W.: Cycling and Accumulation of Biogenic Silica and Organic Matter in High-Latitude Environments: The Ross Sea, oceanog, 5, 146–153, https://doi.org/10.5670/oceanog.1992.03, 1992.

Deng, Y., Guo, Q., Liu, C., He, G., Cao, J., Liao, J., Liu, C., Wang, H., Zhou, J., Liu, Y., Wang, F., Zhao, B., Wei, R., Zhu, J., and Qiu, H.: Early diagenetic control on the enrichment and fractionation of rare earth elements in deep-sea sediments, Science advances, 8, eabn5466, https://doi.org/10.1126/sciadv.abn5466, 2022.

Doe, B. R.: Lead Isotopes, Springer Berlin Heidelberg, Berlin, Heidelberg, 1970.

El-Sayed, S. Z.: Productivity of the southern ocean: a closer look, Comparative Biochemistry and Physiology Part B: Comparative Biochemistry, 90, 489–498, https://doi.org/10.1016/0305-0491(88)90287-8, 1988.

Erhardt, A. M., Douglas, G., Jacobson, A. D., Wimpenny, J., Yin, Q.-Z., and Paytan, A.: Assessing Sedimentary Detrital Pb Isotopes as a Dust Tracer in the Pacific Ocean, Paleoceanog and Paleoclimatol, 36, https://doi.org/10.1029/2020PA004144, 2021.

Gili, S., Gaiero, D. M., Goldstein, S. L., Chemale Jr, F., Koester, E., Jweda, J., Vallelonga, P., and Kaplan, M. R.: Provenance of dust to Antarctica: A lead isotopic perspective, Geophysical Research Letters, 43, 2291–2298, https://doi.org/10.1002/2016GL068244, 2016.

Gobeil, C., Macdonald, R. W., Smith, J. N., and Beaudin, L.: Atlantic water flow pathways revealed by lead contamination in Arctic basin sediments, Science (New York, N.Y.), 293, 1301–1304, https://doi.org/10.1126/science.1062167, 2001.

Griffiths, A., Leung, Y.-L., Bowie, A. R., East, M., Rehkämper, M., and van de Flierdt, T.: Pathways and processes controlling the distribution of anthropogenic lead in the interior of the Southern Ocean, Geochimica et Cosmochimica Acta, 424, 158–175, https://doi.org/10.1016/j.gca.2026.05.019, 2026.

Hamelin, B., Grousset, F., and Sholkovitz, E. R.: Pb isotopes in surficial pelagic sediments from the North Atlantic, Geochimica et Cosmochimica Acta, 54, 37–47, https://doi.org/10.1016/0016-7037(90)90193-O, 1990.

Harlavan, Y. and Erel, Y.: The release of Pb and REE from granitoids by the dissolution of accessory phases, Geochimica et Cosmochimica Acta, 66, 837–848, https://doi.org/10.1016/S0016-7037(01)00806-7, 2002.

https://doi.org/10.5194/egusphere-2026-3608
Preprint. Discussion started: 30 June 2026

Henderson, G. M. and Maier-Reimer, E.: Advection and removal of 210Pb and stable Pb isotopes in the oceans: a general circulation model study, Geochimica et Cosmochimica Acta, 66, 257–272, https://doi.org/10.1016/S0016-7037(01)00779-7, 2002.

Hesse, R. and Schacht, U.: Early Diagenesis of Deep-Sea Sediments, 63, 557–713, https://doi.org/10.1016/B978-0-444-53000-4.00009-3, 2011.

Homoky, W. B., Weber, T., Berelson, W. M., Conway, T. M., Henderson, G. M., van Hulten, M., Jeandel, C., Severmann, S., and Tagliabue, A.: Quantifying trace element and isotope fluxes at the ocean-sediment boundary: a review, Philosophical transactions. Series A, Mathematical, physical, and engineering sciences, 374, https://doi.org/10.1098/rsta.2016.0246, 2016.

Howe, J. A., Shimmield, T. M., and Diaz, R.: Deep-water sedimentary environments of the northwestern Weddell Sea and South Sandwich Islands, Antarctica, Deep Sea Research Part II: Topical Studies in Oceanography, 51, 1489–1514, https://doi.org/10.1016/j.dsr2.2004.07.011, 2004.

Iseki, K.: Particulate Organic Matter Transport to the Deep Sea by Salp Fecal Pellets, Mar. Ecol. Prog. Ser., 5, 55–60, https://doi.org/10.3354/meps005055, 1981.

Izquierdo, M., Tye, A. M., and Chenery, S. R.: Sources, lability and solubility of Pb in alluvial soils of the River Trent catchment, U.K, The Science of the total environment, 433, 110–122, https://doi.org/10.1016/j.scitotenv.2012.06.039, 2012.

Khondoker, R., Weiss, D., van de Flierdt, T., Rehkämper, M., Kreissig, K., Coles, B. J., Strekopytov, S., Humphreys-Williams, E., Dong, S., Bory, A., Bout-Roumazeilles, V., Smichowski, P., Cid-Agüero, P., Babinski, M., Losno, R., and Monna, F.: New constraints on elemental and Pb and Nd isotope compositions of South American and Southern African aerosol sources to the South Atlantic Ocean, Geochemistry, 78, 372–384, https://doi.org/10.1016/j.chemer.2018.05.001, 2018.

Klaas, C.: Expedition Programme PS 133/1 Polarstern: Cape Town - Punta Arenas (01 October 2022 - 17 November 2022), 2022.

Komárek, M., Ettler, V., Chrastný, V., and Mihaljevic, M.: Lead isotopes in environmental sciences: a review, Environment international, 34, 562–577, https://doi.org/10.1016/j.envint.2007.10.005, 2008.

Krisch, S., Olivelli, A., Gerringa, L. J. A., Middag, R., Rogalla, B., and Achterberg, E. P.: The Arctic Ocean is a net sink for anthropogenic lead deposited into the Atlantic Ocean, Nature communications, 16, 11238, https://doi.org/10.1038/s41467-025-67620-9, 2025.

Krishnaswamy, S., Lal, D., Martin, J. M., and Meybeck, M.: Geochronology of lake sediments, Earth and Planetary Science Letters, 11, 407–414, https://doi.org/10.1016/0012-821X(71)90202-0, 1971.

Lalande, C., Nöthig, E.-M., Bauerfeind, E., Hardge, K., Beszczynska-Möller, A., and Fahl, K.: Lateral supply and downward export of particulate matter from upper waters to the seafloor in the deep eastern Fram Strait, Deep Sea Research Part I: Oceanographic Research Papers, 114, 78–89, https://doi.org/10.1016/j.dsr.2016.04.014, 2016.

Lanning, N. T., Jiang, S., Amaral, V. J., Mateos, K., Steffen, J. M., Lam, P. J., Boyle, E. A., and Fitzsimmons, J. N.: Isotopes illustrate vertical transport of anthropogenic Pb by reversible scavenging within Pacific Ocean particle veils, Proceedings of the National Academy of Sciences of the United States of America, 120, e2219688120, https://doi.org/10.1073/pnas.2219688120, 2023.

Larsen, M. M., Blusztajn, J. S., Andersen, O., and Dahllöf, I.: Lead isotopes in marine surface sediments reveal historical use of leaded fuel, Journal of environmental monitoring JEM, 14, 2893–2901, https://doi.org/10.1039/c2em30579h, 2012.

https://doi.org/10.5194/egusphere-2026-3608
Preprint. Discussion started: 30 June 2026

Maccali, J., Hillaire‐Marcel, C., Carignan, J., and Reisberg, L. C.: Pb isotopes and geochemical monitoring of Arctic sedimentary supplies and water mass export through Fram Strait since the Last Glacial Maximum, Paleoceanography, 27, https://doi.org/10.1029/2011PA002152, 2012.

Noble, T. L., Piotrowski, A. M., Robinson, L. F., McManus, J. F., Hillenbrand, C.-D., and Bory, A. J.-M.: Greater supply of Patagonian-sourced detritus and transport by the ACC to the Atlantic sector of the Southern Ocean during the last glacial period, Earth and Planetary Science Letters, 317-318, 374–385, https://doi.org/10.1016/j.epsl.2011.10.007, 2012.

Nriagu, J. O. and Pacyna, J. M.: Quantitative assessment of worldwide contamination of air, water and soils by trace metals, Nature, 333, 134–139, https://doi.org/10.1038/333134a0, 1988.

Oguri, K., Masqué, P., Zabel, M., Stewart, H. A., MacKinnon, G., Rowden, A. A., Berg, P., Wenzhöfer, F., and Glud, R. N.: Sediment Accumulation and Carbon Burial in Four Hadal Trench Systems, JGR Biogeosciences, 127, https://doi.org/10.1029/2022JG006814, 2022.

Olivelli, A., Arcucci, R., Rehkämper, M., and van de Flierdt, T.: Mapping the global distribution of lead and its isotopes in seawater with explainable machine learning, Earth Syst. Sci. Data, 17, 3679–3699, https://doi.org/10.5194/essd-17-3679-2025, 2025.

Olivelli, A., Paul, M., Xu, H., Kreissig, K., Coles, B. J., Moore, R. E., Bridgestock, L., Rijkenberg, M., Middag, R., Lohan, M. C., Weiss, D. J., Rehkämper, M., and van de Flierdt, T.: Vertical transport of anthropogenic lead by reversible scavenging in the South Atlantic Ocean, Earth and Planetary Science Letters, 646, 118980, https://doi.org/10.1016/j.epsl.2024.118980, 2024.

Olivelli, A., Murphy, K., Bridgestock, L., Wilson, D. J., Rijkenberg, M., Middag, R., Weiss, D. J., van de Flierdt, T., and Rehkämper, M.: Decline of anthropogenic lead in South Atlantic Ocean surface waters from 1990 to 2011: New constraints from concentration and isotope data, Marine pollution bulletin, 189, 114798, https://doi.org/10.1016/j.marpolbul.2023.114798, 2023.

Omand, M. M., Govindarajan, R., He, J., and Mahadevan, A.: Sinking flux of particulate organic matter in the oceans: Sensitivity to particle characteristics, Scientific reports, 10, 5582, https://doi.org/10.1038/s41598-020-60424-5, 2020.

Pichevin, L. E., Ganeshram, R. S., Geibert, W., Thunell, R., and Hinton, R.: Silica burial enhanced by iron limitation in oceanic upwelling margins, Nature Geosci, 7, 541–546, https://doi.org/10.1038/NGEO2181, 2014.

Ren, P., Schmidt, B. V., Liu, Q., Wang, S., Liu, X., Liu, K., and Shi, D.: Fractionation of toxic metal Pb from truly dissolved and colloidal phases of seaward rivers in a coastal delta, Front. Mar. Sci., 9, https://doi.org/10.3389/fmars.2022.1085142, 2023.

Ripperger, S., Rehkämper, M., Porcelli, D., and Halliday, A. N.: Cadmium isotope fractionation in seawater — A signature of biological activity, Earth and Planetary Science Letters, 261, 670–684, https://doi.org/10.1016/j.epsl.2007.07.034, 2007.

Ryba, S. A. and Burgess, R. M.: Effects of sample preparation on the measurement of organic carbon, hydrogen, nitrogen, sulfur, and oxygen concentrations in marine sediments, Chemosphere, 48, 139–147, https://doi.org/10.1016/S0045-6535(02)00027-9, 2002.

Samanta, S., Cloete, R., Dey, S. P., Barraqueta, J.-L. M., Loock, J. C., Meynecke, J.-O., Bie, J. de, Vichi, M., and Roychoudhury, A. N.: Exchange of Pb from Indian to Atlantic Ocean is driven by Agulhas current and atmospheric Pb input from South Africa, Scientific reports, 13, 5465, https://doi.org/10.1038/s41598-023-32613-5, 2023.

https://doi.org/10.5194/egusphere-2026-3608
Preprint. Discussion started: 30 June 2026

Schlosser, C. and Garbe-Schönberg, D.: Mechanisms of Pb supply and removal in two remote (sub-)polar ocean regions, Marine pollution bulletin, 149, 110659, https://doi.org/10.1016/j.marpolbul.2019.110659, 2019.

Schlosser, C., Karstensen, J., and Woodward, E. M. S.: Distribution of dissolved and leachable particulate Pb in the water column along the GEOTRACES section GA10 in the South Atlantic, Deep Sea Research Part I: Oceanographic Research Papers, 148, 132–142, https://doi.org/10.1016/j.dsr.2019.05.001, 2019.

Shi, C., He, H., Xia, Z., Gan, H., Xue, Q., Cui, Z., and Chen, J.: Heavy metals and Pb isotopes in a marine sediment core record environmental changes and anthropogenic activities in the Pearl River Delta over a century, The Science of the total environment, 814, 151934, https://doi.org/10.1016/j.scitotenv.2021.151934, 2022.

Soppa, M., Völker, C., and Bracher, A.: Diatom Phenology in the Southern Ocean: Mean Patterns, Trends and the Role of Climate Oscillations, Remote Sensing, 8, 420, https://doi.org/10.3390/rs8050420, 2016.

Stief, P., Schauberger, C., Becker, K. W., Elvert, M., Balmonte, J. P., Franco-Cisterna, B., Middelboe, M., and Glud, R. N.: Hydrostatic pressure induces transformations in the organic matter and microbial community composition of marine snow particles, Commun Earth Environ, 4, https://doi.org/10.1038/s43247-023-01045-4, 2023.

Tanguy, V., Waeles, M., Gigault, J., Cabon, J.-Y., Quentel, F., and Riso, R. D.: The removal of colloidal lead during estuarine mixing: seasonal variations and importance of iron oxides and humic substances, Marine and Freshwater Research, 62, 329–341, https://doi.org/10.1071/MF10220, 2011.

Tréguer, P. J., Sutton, J. N., Brzezinski, M., Charette, M. A., Devries, T., Dutkiewicz, S., Ehlert, C., Hawkings, J., Leynaert, A., Liu, S. M., Llopis Monferrer, N., López-Acosta, M., Maldonado, M., Rahman, S., Ran, L., and Rouxel, O.: Reviews and syntheses: The biogeochemical cycle of silicon in the modern ocean, Biogeosciences, 18, 1269–1289, https://doi.org/10.5194/bg-18-1269-2021, 2021.

Tsunogai, S., Yonemaru, I., and Kusakabe, M.: Post depositional migration of Cu, Zn, Ni, Co, Pb and Ba in deep sea sediments, Geochem. J., 13, 239–252, https://doi.org/10.2343/geochemj.13.239, 1979.

Turekian, K. K.: The fate of metals in the oceans, Geochimica et Cosmochimica Acta, 41, 1139–1144, https://doi.org/10.1016/0016-7037(77)90109-0, 1977.

van de Flierdt, T., Frank, M., Halliday, A. N., Hein, J. R., Hattendorf, B., Günther, D., and Kubik, P. W.: Lead isotopes in North Pacific deep water – implications for past changes in input sources and circulation patterns, Earth and Planetary Science Letters, 209, 149–164, https://doi.org/10.1016/S0012-821X(03)00069-4, 2003.

Veron, A. J., Church, T. M., Flegal, A. R., Patterson, C. C., and Erel, Y.: Response of lead cycling in the surface Sargasso Sea to changes in tropospheric input, J. Geophys. Res., 98, 18269–18276, https://doi.org/10.1029/93JC01639, 1993.

Weis, J., Chase, Z., Schallenberg, C., Strutton, P. G., Bowie, A. R., and Fiddes, S. L.: One-third of Southern Ocean productivity is supported by dust deposition, Nature, 629, 603–608, https://doi.org/10.1038/s41586-024-07366-4, 2024.

Weiss, D., Boyle, E. A., Wu, J., Chavagnac, V., Michel, A., and Reuer, M. K.: Spatial and temporal evolution of lead isotope ratios in the North Atlantic Ocean between 1981 and 1989, J. Geophys. Res., 108, https://doi.org/10.1029/2000JC000762, 2003.

Winter, B. L., Johnson, C. M., and Clark, D. L.: Strontium, neodymium, and lead isotope variations of authigenic and silicate sediment components from the Late Cenozoic Arctic Ocean: Implications for sediment provenance and the source of trace metals in seawater, Geochimica et Cosmochimica Acta, 61, 4181–4200, https://doi.org/10.1016/S0016-7037(97)00215-9, 1997.

https://doi.org/10.5194/egusphere-2026-3608
Preprint. Discussion started: 30 June 2026

Yang, S.-C., Hawco, N. J., Pinedo-González, P., Bian, X., Huang, K.-F., Zhang, R., and John, S. G.: A new purification method for Ni and Cu stable isotopes in seawater provides evidence for widespread Ni isotope fractionation by phytoplankton in the North Pacific, Chemical Geology, 547, 119662, https://doi.org/10.1016/j.chemgeo.2020.119662, 2020.

Yang, W., Guo, L., Chuang, C.-Y., Santschi, P. H., Schumann, D., and Ayranov, M.: Influence of organic matter on the adsorption of 210Pb, 210Po and 7Be and their fractionation on nanoparticles in seawater, Earth and Planetary Science Letters, 423, 193–201, https://doi.org/10.1016/j.epsl.2015.05.007, 2015.

Zhao, S., Feng, C., Wang, D., Liu, Y., and Shen, Z.: Salinity increases the mobility of Cd, Cu, Mn, and Pb in the sediments of Yangtze Estuary: relative role of sediments' properties and metal speciation, Chemosphere, 91, 977–984, https://doi.org/10.1016/j.chemosphere.2013.02.001, 2013.

Zurbrick, C. M., Gallon, C., and Flegal, A. R.: Historic and Industrial Lead within the Northwest Pacific Ocean Evidenced by Lead Isotopes in Seawater, Environmental science & technology, 51, 1203–1212, https://doi.org/10.1021/acs.est.6b04666, 2017.